Talanta 79 (2009) 97–102

Contents lists available at ScienceDirect

Talanta

journal homepage: www.elsevier.com/locate/talanta

A novel amperometric biosensor for the detection of nitrophenol

A.K.M. Kafi, Aicheng Chen*

Department of Chemistry, Lakehead University, 955 Oliver Road, Thunder Bay, Ontario P7B 5E1, Canada

ARTICLE INFO

Article history:
Received 19 December 2008
Received in revised form 4 March 2009
Accepted 5 March 2009
Available online 19 March 2009

Keywords:
Nitrophenol
HRP
Biosensors
TiO_2 nanotube arrays
Methylene blue

ABSTRACT

We report on a novel amperometric biosensor for detecting phenolic compounds based on the co-immobilization of horseradish-peroxidase (HRP) and methylene blue (MB) with chitosan on Au-modified TiO_2 nanotube arrays. The titania nanotube arrays were directly grown on a Ti substrate using anodic oxidation first; a gold thin film was then coated onto the TiO_2 nanotubes by an argon plasma technique. The morphology and composition of the fabricated Au-modified TiO_2 nanotube arrays were characterized by scanning electron microscopy (SEM) and energy-dispersive X-ray spectroscopy (EDS). Cyclic voltammetry and amperometry were used to study the proposed electrochemical biosensor. The effect of pH, applied electrode potential and the concentration of H_2O_2 on the sensitivity of the biosensor have been systemically investigated. The performance of the proposed biosensor was tested using seven different phenolic compounds, showing very high sensitivity; in particular, the linearity of the biosensor for the detection of 3-nitrophenol was observed from 3×10^{-7} to 1.2×10^{-4} M with a detection limit of 9×10^{-8} M (based on the S/N = 3).

1. Introduction

Phenolic compounds are widely used in the chemical industry and, when released into the environment, are considered to be very toxic to both humans and the environment [1–3]. This class of compounds includes highly poisonous, caustic substances derived from coal tar and the production of plastics, dyes, pharmaceuticals, germicides, preservatives and antiseptics. Phenolic compounds are listed by the Agency for Toxic Substances and Disease Registry (ATSDR) as priority hazardous substances. Approximately 165 phenolic compounds are known to have a toxic effect on the environment; among them, nitrophenols are considered as major toxic pollutants. The detection of phenolic compounds is thus very important for measuring toxicity in the environment. Some noticeable detection techniques, such as gas chromatography, liquid chromatography and spectrophotometry, have been employed to determine the presence of phenol and its derivatives [4–7]. However, these methods are time-consuming and require tedious sample preparation and expensive equipment; they are difficult to use for in situ detection in the field. Methods for screening these compounds in the field are of considerable value. The development of in situ enzyme-based electrochemical biosensors has attracted great attention [8–10]. Tyrosinase is the most widely used enzyme for the detection of phenolic compounds [11–14]. However, tyrosinase-based biosensors are limited to the monitoring of phenolic compounds with at least one free *ortho*-position. In addition, tyrosinase-based biosensors show no response to nitrophenol [15]. Therefore, there is great interest in developing electrochemical techniques and other enzyme-based biosensors for the determination of nitrophenols.

It is well known that the major drawbacks inherent to enzyme-based sensors include the difficulty in enzyme immobilization and their limited lifetime due to the desorption and/or deactivation of the immobilized enzymes. The performance of a biosensor mainly depends on the properties of the bioactive layer associated with the transducer [16–20]. It is crucial to retain a high electroactivity of the protein or enzyme immobilized on the electrode surface. Different matrices have been used for the immobilization of HRP [21–23]. Nanostructured materials have been attracting considerable attention because of their regular structure and high active surface area for protein binding [24–27]. Titanium dioxide has been widely used as a photocatalyst and is promising for biosensor design due to its nontoxicity, low cost and high chemical and thermal stability [28–31]. In this paper, we report on a novel nitrophenol biosensor based on the co-immobilization of HRP and methylene blue (MB) with chitosan on Au-modified TiO_2 nanotube arrays. To the best of our knowledge, no electrochemical biosensors have been reported for 3-nitrophenol detection with the exception of one study aimed at developing a *arthrobacter sp.* JS443-based whole cell amperometric biosensor for 4-nitrophenol, where 3-nitrophenol was mentioned as an interfering species [32]. However, the stability of the whole cell based biosensor was very low, losing its response to nitrophenol after 3 days. In this study, the titania nanotubes were fabricated by anodizing titanium foil in a standard two-

* Corresponding author. Tel.: +1 807 3438318; fax: +1 807 3467775.
E-mail address: aicheng.chen@lakeheadu.ca (A. Chen).

0039-9140/$ – see front matter © 2009 Elsevier B.V. All rights reserved.
doi:10.1016/j.talanta.2009.03.015

electrode electrochemical cell containing sodium fluoride (NaF) and hydrofluoric acid (HF). A gold thin film was then uniformly coated on the TiO_2 nanotubes using a plasma sputtering technique. The immobilization of HRP and MB on the TiO_2 nanotubes arrays was achieved by a casting method. Our electrochemical measurements show that the Au-modified TiO_2 nanotubes arrays provide excellent matrixes for the immobilization of HRP and that the immobilized HRP exhibits high stability and retains high catalytical activity. The amperometric response of the designed biosensor to phenolic compounds concentration shows long range linearity. In addition, our study reveals that the presence of MB significantly enhances the sensitivity of the designed biosensor.

2. Experimental

2.1. Reagents and materials

Horseradish peroxidase (EC1.11.1.7, Type X) was purchased from Sigma-Aldrich and used as received. The HRP stock solutions were stored at a temperature of 4 °C. Mehtylene blue was purchased from British Drug Houses Ltd., Poole, England. Hydrogen Peroxide (30%) was bought from Fluka and the stock solutions of H_2O_2 were diluted from that. Nitrophenols and other phenolic compounds were obtained from Sigma-Aldrich. Hydrofluoric acid (HF, 49%) came from Fisher Chemical and dimethyle sulfoxide (DMSO) from Caledon Laboratories Ltd, Canada. All other reagents were of analytical grade and were used as supplied. Water used to prepare all the solutions in this study was purified with a Nanopure® water system. All experiments were performed in 0.1 M phosphate buffer solution (PBS) with different pH values adjusted with K_2HPO_4 and KH_2PO_4.

2.2. Fabrication of biosensors

The TiO_2 nanotube arrays were synthesized by anodic oxidation of Ti substrates [30,33–35]. Briefly, titanium foils were ultrasonically cleaned in acetone and ethanol prior to anodization. After rinsing with distilled water, a clean titanium foil electrode (0.4 cm × 0.5 cm × 0.05 cm) was first etched in 18% HCl at 85 °C for 10 min. The etched titanium foil was rinsed thoroughly with pure water and then anodized at a direct current (DC) voltage of 40 V in a two-electrode electrochemical cell in an electrolyte containing dimethyl sulfoxide (DMSO) and hydrofluoric acid (HF, 2%) for 8 h. A platinum coil was used as the counter electrode and the experiment was conducted at room temperature. After anodization, samples were rinsed thoroughly with pure water and then ultrasonicated to remove surface debris. In order to improve the crystalline properties and remove the remnants of the barrier oxide layer after the anodic reaction, the samples were annealed at 450 °C for 1 h. The Au thin film was then coated onto the TiO_2 nanotube arrays by argon plasma sputtering for 30 s. Finally, 20 μL of 2 mg/mL of HRP and 20 μL of 1 mg/mL of MB and 10 μL of 2 mg/mL of chitosan were co-immobilized onto the synthesized Au-coated TiO_2 nanotube arrays ($Ti/TiO_2/Au/HRP$-MB). Chitosan was used here because of its excellent membrane-forming ability, good adhesion, biocompatibility, nontoxicity and high mechanical strength, which make the biosensor more stable [36]. For comparison, a biosensor based on TiO_2/Au without MB ($Ti/TiO_2/Au/HRP$) and TiO_2 nanotube arrays without the Au thin film ($Ti/TiO_2/HRP$) were also fabricated. All resulting electrodes were stored in 0.1 M PBS (pH 7.0) and at 4 °C when not in use.

2.3. Instrument and electrochemical measurements

The morphology and the composition of the synthesized TiO_2 nanotube arrays were characterized by scanning electron microscope (SEM) (JEOL JSM 5900 LV), at an acceleration voltage of 13 kV, and an energy-dispersive X-ray (EDX) spectrometer. Electrochemical measurements were carried out with a CHI (630B) workstation. A three-electrode configuration was employed for these experiments. The fabricated biosensors were employed as the working electrodes. A platinum coil was connected as the counter electrode and a KCl saturated Ag/AgCl electrode was used as the reference electrode. Cyclic voltammetric measurements were carried out in 0.1 M PBS by applying 0.0 to −0.8 V vs. Ag/AgCl sweep range in the negative scanning direction. Amperometric responses were measured in a stirred cell by applying a potential of −0.05 V to the working electrode. A magnetic stirrer was used for this experiment. All measurements were performed at room temperature.

3. Results and discussion

3.1. Structural characterization of TiO_2 nanotube arrays

The morphology and composition of the Ti substrate after anodization were examined by SEM observation and EDS analysis. Fig. 1A shows a typical SEM image of the TiO_2 nanotube arrays with a sputtered Au thin film as fabricated in this study. The TiO_2 nanotube arrays were directly grown on the Ti substrate by anodizing the Ti substrate in the electrolyte containing DMSO and 2% HF at 40 V for 8 h. The typical dimensions are calculated to be ~90 nm outer diameter, ~70 nm inner diameter, ~20 nm wall-thickness. Fig. 1B shows the EDS spectrum of the Au-modified nanotube arrays. Both Ti and O peaks are observed, and the ratio of Ti to O is close to 1:2, confirming that the formed nanotubes are TiO_2. The strong Au peak is derived from the Au thin film sputtered on the TiO_2 nanotube arrays. The adhesion and integrity of the synthesized TiO_2 nanotube layer are essential for the effective immobilization of biomolecules.

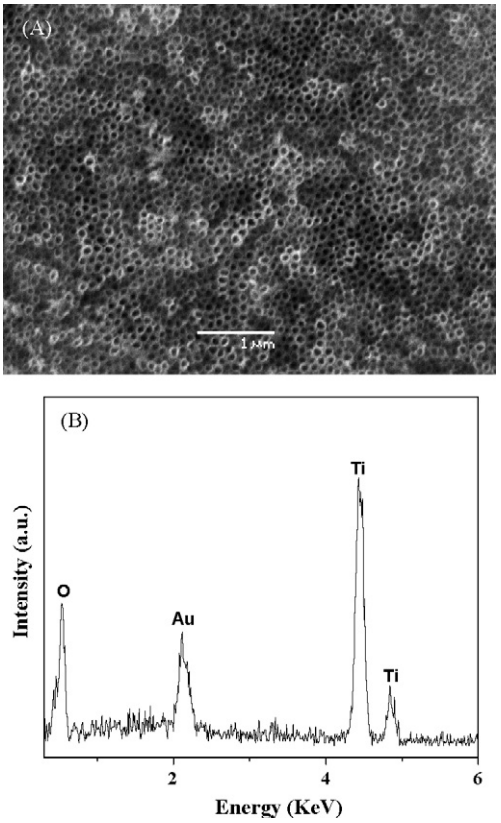

Fig. 1. (A) SEM image of TiO_2 nanotube arrays directly grown on Ti substrates, (B) EDS spectrum of Au-modified TiO_2 nanotube arrays.

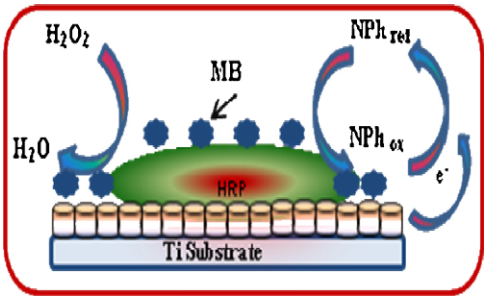

Scheme 1. Schematic diagram of the biosensor in response to nitrophenol.

This anodization method is preferable to other methods such as sol–gel and electrophoretic deposition because the TiO_2 layer is directly grown on the Ti substrate, thus exhibiting much better adhesion to the Ti substrate than that of other methods [37]. Since the TiO_2 nanotube arrays make a tightly adherent surface layer on the Ti substrate and, by taking in all other considerations such as non-toxicity, high surface area and strong thermal and chemical stability, it can be seen that the synthesized TiO_2 nanotube arrays are promising for biosensing applications.

3.2. The principle of HRP-modified electrodes for phenolic compounds detection

It has been reported that peroxidase cycles of HRP can be activated by H_2O_2 to generate active oxyferryl radicals [38]. The immobilized peroxidase on an electrode surface can be reduced to its native state by direct or mediated electron transfer in encountering phenol, aromatic amines, ferrocenes, and amine ruthenium complexes [39–42]. The response of a phenolic biosensor is based on the double displacement mechanism in which two substrates, peroxide (normally H_2O_2) and the given phenolic compounds, are involved [43]. The structure of the electrode developed in the present work as well as the enzymatic mechanism used to create a biosensor based on HRP for phenolic compound detection is proposed in Scheme 1. The reactions consist of the oxidation of the heme group of HRP molecules by H_2O_2 and the reduction by the phenolic compound. In the latter reaction, the phenolic compounds are mainly converted into free radical products which are electroactive and can be electrochemically reduced on the electrode surface [10]. The resulting reduction current is proportional to the concentration of phenolic compounds in solution as long as the H_2O_2 concentration is not limiting.

3.3. CV of the modified electrodes

Fig. 2 shows the cyclic voltammograms (CVs) of the Ti/TiO_2 (dashed line) and $Ti/TiO_2/Au$ (solid line) electrodes recorded in a 0.1 M KCl + 5.0×10^{-3} M $Fe(CN)_6^{3-/4-}$ solution at a sweep rate of 50 mV/s. TiO_2 is a semiconductor and its electrical conductivity is relatively low. As expected, neither an oxidation nor reduction peak is observed in the CV of the Ti/TiO_2 electrode. However, a well-defined and large pair of oxidation peaks located at 0.35 V, and a reduction peak centered at 0.1 V appear in the CV of the $Ti/TiO_2/Au$ electrode. The above results show that the presence of the Au thin film significantly increases the electrical activity of the TiO_2 nanotube arrays.

3.4. Biosensor behavior

As seen in Scheme 1, H_2O_2 plays an important role in the detection of phenolic compounds. Before we tested the prepared biosensor for nitrophenols detection, we studied its response to

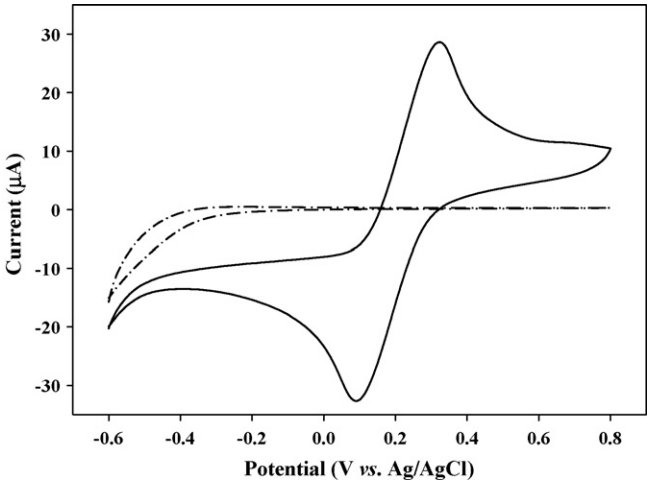

Fig. 2. Cyclic voltammamograms of the Ti/TiO_2 (dashed line) and $Ti/TiO_2/Au$ (solid line) electrodes recorded in 5×10^{-3} M $Fe(CN)_6^{3-/4-}$ + 0.1 M KCl solution at a scan rate of 50 mV/s.

H_2O_2. Fig. 3 compares the CV curves of the $Ti/TiO_2/Au/HRP/MB$ electrode in 0.1 M PBS (pH 7.0) in the presence of 3.0×10^{-3} M H_2O_2 (solid line) and in the absence of H_2O_2 (dashed line) at a scan rate of 50 mV/s, showing that the prepared biosensor has a strong response to H_2O_2. To reveal the effect of methylene blue, the CVs of the $Ti/TiO_2/Au/HRP$ electrode in the absence of (dotted line) and in the presence of 3.0×10^{-3} M H_2O_2 (dashed line) in 0.1 M PBS (pH 7.0) at a scan rate of 50 mV/s are presented in the inset of Fig. 3. The current response of the $Ti/TiO_2/Au/HRP$-MB electrode is ~120% higher for H_2O_2 reduction than that of the $Ti/TiO_2/Au/HRP$ electrode, demonstrating that MB plays an important role as an electron mediator.

Fig. 4 shows the linear sweep voltammograms of the $Ti/TiO_2/Au/HRP$-MB electrode scanned from −0.3 to +0.3 V in various solutions (a–e). Comparison of Curve a and b shows that there is almost no increase in amperometric current for this biosensor when only 3-NPh was introduced into the electrolyte. The amperometric current slightly increases while only H_2O_2 was injected (Curve c), due to the catalytic reduction of H_2O_2 on the electrode. Interestingly, when both 3-NPh and H_2O_2 were added (Curve d), a high amperometric current appears, indicating the presence of

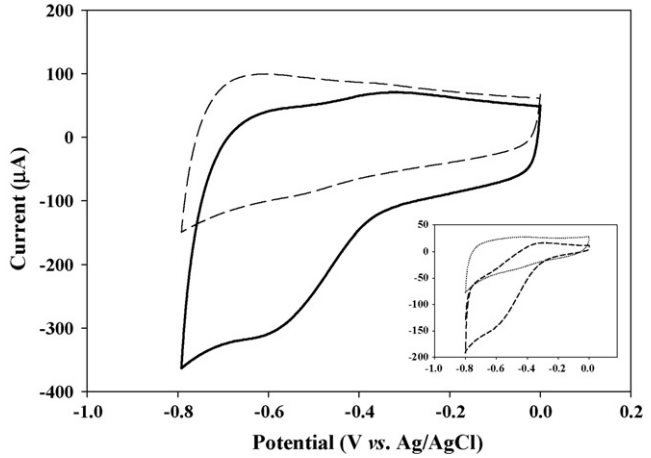

Fig. 3. Cyclic voltammamograms of the $Ti/TiO_2/Au/HRP$-MB electrode in the absence (dashed) and presence (solid) of 3×10^{-3} M H_2O_2 in 0.1 M PBS (pH 7.0) at a scan rate of 50 mV/s. The inset shows the CVs of $Ti/TiO_2/Au/HRP$ in the absence (dotted line) and presence (dashed line) of 3×10^{-3} M H_2O_2 in 0.1 M PBS (pH 7.0) at a scan rate of 50 mV/s.

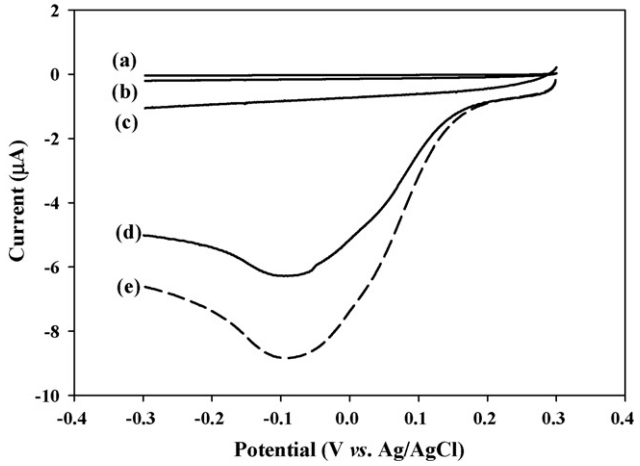

Fig. 4. Linear sweep voltammograms of the Ti/TiO_2/Au/HRP-MB electrode recorded (a) in the blank solution 0.1 M PBS (pH 7.0); (b) in the presence of 2.5×10^{-5} M 3-nitrophenol; (c) in the presence of 2.5×10^{-5} M H_2O_2; (d) in the presence of 2.5×10^{-5} M 3-nitrophenol and 2.5×10^{-5} M H_2O_2; (e) in the presence of 5×10^{-5} M 3-nitrophenol and 2.5×10^{-5} M H_2O_2.

H_2O_2 is necessary for the detection of 3-NPh. When we increase the concentration of 3-NPh to 5.0×10^{-5} M 3-NPh, the amperometric current is further increased (Curve e), showing that 3-NPh is responsible for this enhanced current. The high sensitivity observed at the Ti/TiO_2/Au/HRP-MB electrode for 3-NPh indicates that the electron mediator MB greatly accelerates the electron transfer [28].

3.5. Optimal parameters

The effect of an applied potential on the amperometric response of the biosensor was investigated. Fig. 5A shows the influence of applied potential on the biosensor response to 3-NPh. The biosensor exhibits a maximum current at −0.05 V when the electrode potential was changed from −0.3 V to 0.1 V. As mentioned in Section 3.2, the biosensing mechanism consists of the oxidation of the heme group of HRP molecules by H_2O_2 and the reduction by nitrophenol. In the latter reaction, the nitrophenol is converted into radical intermediates which are electroactive and can be electrochemically reduced on the electrode surface. The decrease of the current is likely due to the polymerization of the formed radicals at the more negative potentials.

A similar effect was also observed for the tyrosinase-based biosensors for catechol and phenol [44,45].

It is known that the presence of a high concentration of H_2O_2 results in inhibition of enzyme activity [37,46]. To achieve high sensitivity and avoid the formation of inactive enzymes caused by high concentrations of H_2O_2, we studied the effect of the H_2O_2 concentration on the Ti/TiO_2/Au/HRP-MB biosensor in 0.1 M PBS (pH 7.0) containing 25 μM 3-NPh under the optimized electrode potential −0.05 V as shown in Fig. 5B. This reveals that the maximum amperometric response was achieved in the presence of 20 μM H_2O_2. We further investigated the effect of the solution's pH on the biosensor response. The influence of pH was evaluated over the pH range of 3.0 to 9.0. As shown in Fig. 5C, a much lower response was obtained in the case of pH lower than 6.0 or higher than 8.0, showing that pH 7.0 is the optimum solution pH for the biosensor fabricated in this study.

3.6. Amperometric response of the biosensor

The amperometric response of the Ti/TiO_2/Au/HRP-MB biosensor was tested in a stirred cell containing 0.1 M PBS (pH 7.0) under the optimized operating electrode potential of −0.05 V. For comparison, Fig. 6A presents the typical amperometric responses of three different electrodes (a–c) in the presence of 2×10^{-5} M H_2O_2 for successive additions of 3-NPh. The corresponding calibration plots for the three amperometric response curves are shown in Fig. 6B. The amperometric response of the Ti/TiO_2/Au/HRP electrode (Curve b) to 3-NPh is much higher than that of the Ti/TiO_2/HRP

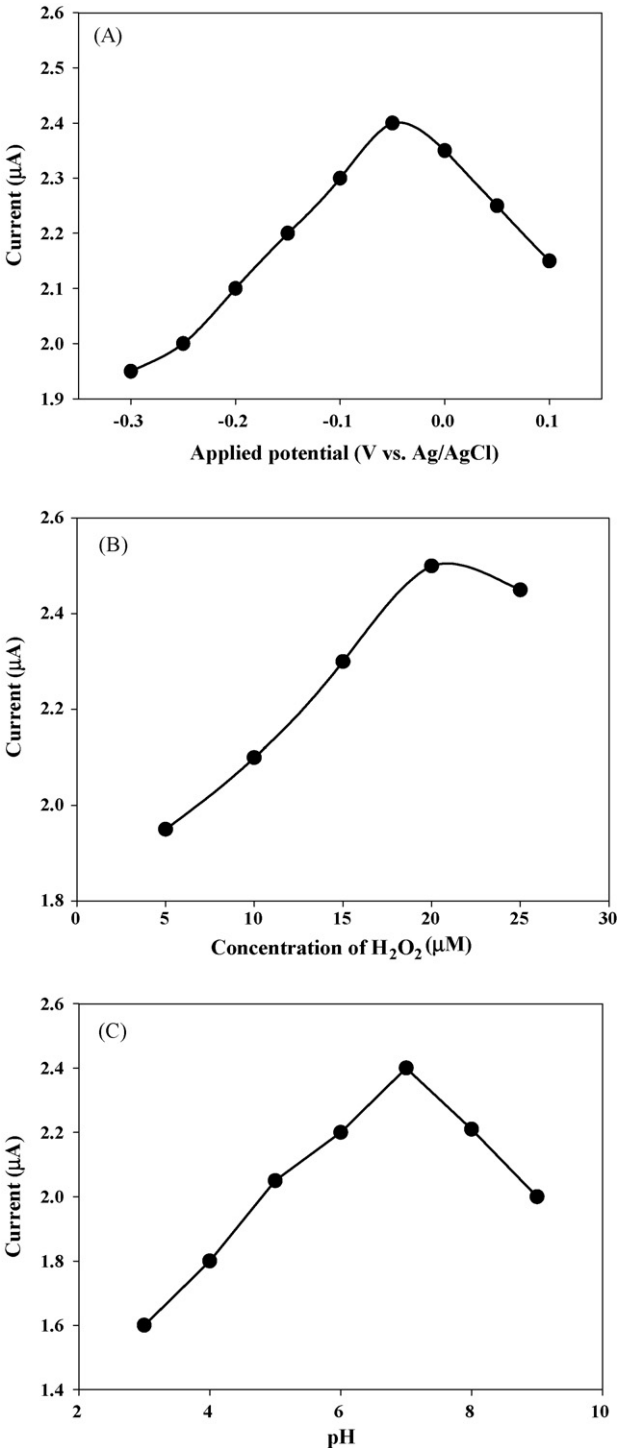

Fig. 5. (A) Dependence of catalytic current of the biosensor at different applied potentials measured in a pH 7.0 PBS containing 2.5×10^{-5} M 3-nitrophenol and 2.5×10^{-5} M H_2O_2. (B) Effect of the H_2O_2 concentration on the amperometric response of the Ti/TiO_2/Au/HRP-MB electrode to 2.5×10^{-5} M 3-nitrophenol in 0.1 M PBS (pH 7.0) at the potential of -0.05 V; (C) influence of pH on the catalytic current of the biosensor in the presence of 2.5×10^{-5} M 3-nitrophenol in 0.1 M PBS containing 2×10^{-5} M H_2O_2 at the potential of −0.05 V.

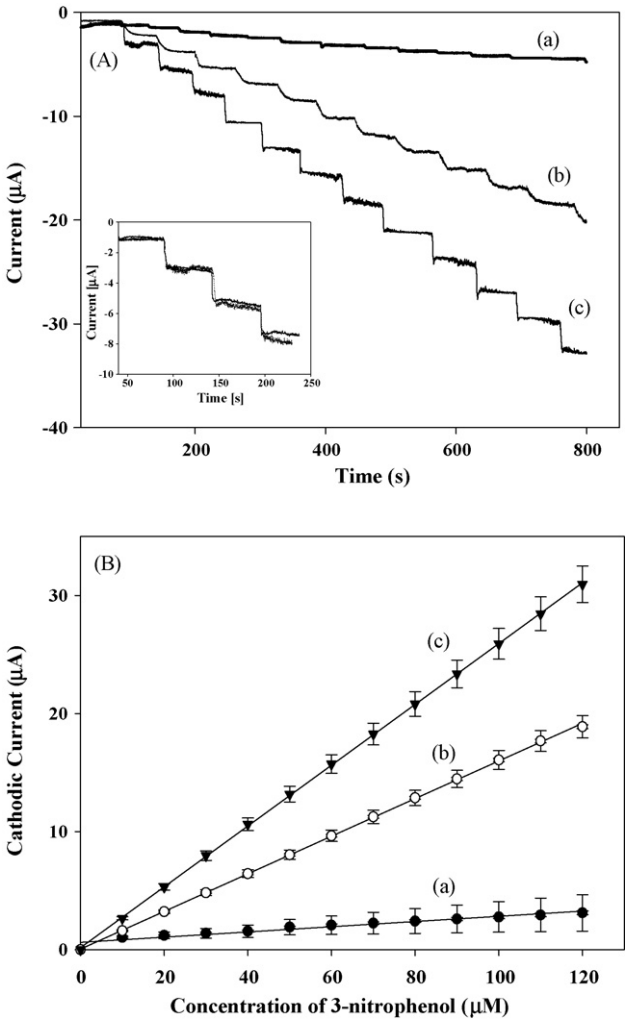

Fig. 6. (A) Typical amperometric response of the Ti/TiO_2/HRP (a), Ti/TiO_2/Au/HRP (b), and Ti/TiO_2/Au/HRP-MB (c) electrodes with successive additions of 1×10^{-5} M 3-nitrophenol in 0.1 M PBS (pH 7.0) in the presence of 2×10^{-5} M H_2O_2 at the operating potential of −0.05 V. Inset: the amperometric response of the Ti/TiO_2/Au/HRP-MB electrode after 45 days under same experimental conditions (solid line); (B) calibration plots of the proposed biosensors (the same experimental conditions as in A).

electrode (Curve a). The presence of MB on the electrode surface (Curve c) further increases the response of the biosensor. As seen in Curve c, the response of the Ti/TiO_2/Au/HRP-MB biosensor is very quick; over 95% of the steady state current is achieved within 5 s. Under these optimized experimental parameters, the Ti/TiO_2/Au/HRP-MB biosensor fabricated in this study shows a linear response in the range of 3×10^{-7} to 1.2×10^{-4} M 3-NPh with a correlation coefficient of 0.993 and very high sensitivity (0.35 μA/μM). This is 87 times higher than the *arthrobacter sp.* JS443-based whole cell amperometric biosensor [32]. The detection limit is estimated to be 9×10^{-8} M 3-NPh (based on S/N = 3). The performance of the Ti/TiO_2/Au/HRP-MB biosensor developed in this study has also been tested with six other phenolic compounds: phenol, 2-nitrophenol, 4-nitrophenol, m-cresol, p-cresol and 3-chlorophenol. As summarized in Table 1, the developed Ti/TiO_2/Au/HRP-MB biosensor exhibits a long linear range, high sensitivity and very low detection limit for all the tested phenolic compounds. Further study is needed to improve its selectivity.

3.7. Stability and reproducibility of the biosensor

The long-term stability of this biosensor was also investigated. The Ti/TiO_2/Au/HRP-MB electrode was stored in PBS (pH 7.0) at 4 °C when not being in use. The Ti/TiO_2/Au/HRP-MB biosensor fabricated in this study is extremely stable, and it retains 92% of its initial current response after 45 days as shown in the inset to Fig. 6A (solid line). The repeatability of the biosensor for the established current response was also examined, showing that the relative standard deviation (RSD) was 3.55% for 10 successive measurements with 2×10^{-5} M 3-NPh. To compare the performance of the biosensor fabricated in this study, we searched the literature. On one hand, we did not find any biosensor for 3-nitrophenol detection. To the best of our knowledge, the Ti/TiO_2/Au/HRP-MB electrode developed in this study is the first electrochemical biosensor for 3-nitrophenol detection. On the other hand, we found a number of biosensors for phenol detection in the literature. Table 2 compares the performance of the Ti/TiO_2/Au/HRP-MB biosensor for phenol detection with the reported electrochemical biosensors [15,45,47–50], revealing that the biosensor proposed in this study exhibits a very long linearity, high sensitivity, low detection limit and high stability, very promising for the detection of phenolic compounds.

Table 1
The performance of the biosensor proposed in this study for the detection of different phenolic compounds.

Phenolic compounds	Linear range	Sensitivity (μA/μM)	LOD
Phenol	8×10^{-7} to 1.3×10^{-4} M	0.19 (r = 0.996; n = 15)	1.95×10^{-7} M
2-nitrophenol	4×10^{-7} to 1.4×10^{-4} M	0.29 (r = 0.997; n = 15)	1.20×10^{-7} M
3-nitrophenol	3×10^{-7} to 1.2×10^{-4} M	0.35 (r = 0.993; n = 15)	9.00×10^{-8} M
4-nitrophenol	3×10^{-7} to 1.4×10^{-4} M	0.30 (r = 0.999; n = 15)	1.10×10^{-7} M
m-Cresol	6×10^{-7} to 1.2×10^{-4} M	0.26 (r = 0.991; n = 15)	1.35×10^{-7} M
p-Cresol	8×10^{-7} to 1.1×10^{-4} M	0.19 (r = 0.997; n = 15)	1.90×10^{-7} M
3-Chlorophenol	7×10^{-7} to 1.1×10^{-4} M	0.23 (r = 0.996; n = 15)	1.55×10^{-7} M

Table 2
Comparison of the performance of the electrochemical biosensor developed in this study with other biosensors reported in the literature for the detection of phenol.

Immobilization matrix	Linearity	Sensitivity	LOD	Stability	Ref
Tyr/nano-$MgFe_2O_4$–SiO_2	1–250 μM	54.2 mA/M	600 nM	70% (30 days)	15
Tyr/electropolymerized PTS-doped polypyrrole	3.3–220 μM	17.1 μA/mM	8.0×10^{-7} M	80% (90 days)	47
Tyr/Au nanoparticles with GC electrode	1–40 μM	82 μA/mM	2.1×10^{-7} M	N/A	45
Tyr/core-shell magnetic nanoparticles	1–250 μM	54.2 μA/mM	6×10^{-7} M	70% (30 days)	48
Tyr/sonogel-carbon	0.5–30 μM	32 nA/μM	3×10^{-7} M	80% (40 days)	49
HRP/sol–gel with GC	5–50 μM	3.65 nA/μM	8×10^{-7} M	80% (30 days)	50
HRP-TiO_2 nanotube	0.8–130 μM	0.19 μA/μM	2×10^{-7} M	92% (45days)	Proposed

Tyr = Tyrosinase; HRP = Horseradish peroxidase; GC = Glassy carbon.

4. Conclusions

In this paper, we have presented a promising electrochemical biosensor for the detection of phenolic compounds based on the co-immobilization of HRP and MB with chitosan on Au-modified titanium dioxide nanotube arrays. The titania nanotube arrays were directly grown on a titanium substrate by simple anodic oxidation. These titania nanotube arrays possess large surface area and good uniformity, ideal matrixes for enzyme immobilization. The presence of an Au thin film greatly increases the electrical activity of the formed TiO_2 nanotube arrays. Our electrochemical measurements reveal that the immobilized HRP exhibits high biological activity and stability and that the presence of methylene blue further enhances the sensitivity of the designed electrochemical biosensor for phenolic compounds. The developed biosensor exhibits fast amperometric response, high sensitivity, low detection limit and long-time stability for 3-nitrophenol. This study provides proof-of-concept for the development of HRP-based biosensors for the detection of high toxic nitrophenolic pollutants.

Acknowledgments

This work was supported by a Discovery Grant from the Natural Sciences and Engineering Research Council of Canada (NSERC). A.K.M. Kafi acknowledges the Ontario Post Doctoral Fellowship. A. Chen acknowledges NSERC and the Canada Foundation of Innovation (CFI) for the Canada Research Chair Award in Material and Environmental Chemistry.

References

[1] Z. Liu, B. Liu, J. Kong, J. Deng, Anal. Chem. 72 (2000) 4707.
[2] L. Coche-Guerente, P. Labbe, V. Mengeaud, Anal. Chem. 73 (2001) 3206.
[3] J. Febortova, V. Tatarvicova, Analyst 119 (1994) 1519.
[4] A.J.H. Louter, P.A. Jonse, J.D. Jorritsma, J.J. Vreuls, U.A.T. Brinkman, Chromatography 20 (1997) 363.
[5] O. Jauregui, M.T. Galceran, Anal. Chim. Acta 340 (1997) 191.
[6] E. Orejuela, M. Silva, Analyst 127 (2002) 127.
[7] V. Janda, K. Krijit, J. Chromatogr. 283 (1984) 309.
[8] F.D. Munteanu, A. Lindgren, J. Emneus, L. Gorton, T. Ruzgas, E. Csoregi, A. Ciucu, A. Van, R.B. Huystee, I.G. Gazaryan, L.M. Lagrimini, Anal. Chem. 70 (1998) 2596.
[9] S.S. Rosatto, L.T. Kubota, G.O. Neto, Anal. Chim. Acta 390 (1999) 65.
[10] X.J. Wu, M.M.F. Choi, X.M. Wu, Analyst 129 (2004) 1143.
[11] B. Wang, J. Zhang, S. Dong, Biosens. Bioelectron. 15 (2001) 397.
[12] C. Védrine, S. Fabiano, C. Tran-Minh, Talanta 59 (2003) 535.
[13] J. Abdullah, M. Ahmad, L.Y. Heng, N. Karuppiah, H. Sidek, Talanta 70 (2006) 527.
[14] L.D. Mello, M.D.P.T. Sotomayor, L.T. Kubota, Sens. Actuators B: Chem. 96 (2003) 636.
[15] Z.J. Liu, B.H. Liu, J.L. Kong, J.Q. Deng, Anal. Chem. 72 (2000) 4707.
[16] S. Liu, L. Bakovic, A. Chen, J. Electroanal. Chem. 591 (2006) 210.
[17] Y. Jung, J.Y. Jeong, B.H. Chung, Analyst 133 (2008) 697.
[18] T.P. Rao, R. Kala, Talanta 76 (2008) 485.
[19] S. Liu, B. Miller, A. Chen, Electrochem. Commun. 7 (2005) 1232.
[20] A. Ramanavicius, A. Kausaite, A. Ramanaviciene, Analyst 133 (2008) 1083.
[21] S. Korkut, B. Keskinler, E. Erhan, Talanta 76 (2008) 1147.
[22] M. Tian, N. Kanavillil, L. Davey, K.T. Leung, H. Schraft, A. Chen, J. Electroanal. Chem. 611 (2007) 133.
[23] Y.T. Kong, M. Boopathi, Y.B. Shim, Biosens. Bioelectron. 19 (2003) 227.
[24] J. Wang, M. Musameh, Y. Lin, J. Am. Chem. Soc. 125 (2003) 2408.
[25] W. Tremel, Angew. Chem. Int. Ed. 38 (1999) 2175.
[26] Y. Coffinier, S. Janel, A. Addad, R. Blossey, L. Gengembre, E. Payen, R. Boukherroub, Langmuir 23 (2007) 1608.
[27] K.B. Male, S. Hrapovic, J.H.T. Luong, Analyst 132 (2007) 1254.
[28] A.K.M. Kafi, G. Wu, A. Chen, Biosens. Bioelectron. 24 (2008) 566.
[29] G. Wu, T. Nishikawa, B. Ohtani, A. Chen, Chem. Mater. 19 (2007) 4530.
[30] S. Yoriya, M. Paulose, O.K. Varghese, G.K. Mor, C.A. Grimes, J. Phys. Chem. C 111 (2007) 13770.
[31] S. Liu, A. Chen, Langmuir 21 (2005) 8409.
[32] Y. Lei, P. Mulchandani, W. Chen, J. Wang, A. Mulchandani, Electroanalysis 16 (2004) 2030.
[33] C. Richter, E. Panaitescu, R.J. Welly, L. Menon, J. Nanosci. Nanotechnol. 22 (2007) 1624.
[34] A. Ghicov, J.M. Macak, H. Tsuchiya, J. Kunze, V. Haeublein, L. Frey, P. Schmuki, Nano Lett. 6 (2006) 1080.
[35] M. Tian, G. Wu, B. Adams, J. Wen, A. Chen, J. Phys. Chem. C 112 (2008) 825.
[36] X.L. Luo, J.J. Xu, Q. Zhang, G.J. Yang, H.Y. Chen, Biosens. Bioelectron. 21 (2005) 190.
[37] X.F. Xiao, T. Tian, R.F. Liu, H.D. She, Mater. Chem. Phys. 106 (2007) 27.
[38] S.I. Imabayashi, Y.T. Kong, M. Watanabe, Electroanalysis 13 (2001) 408.
[39] B. Dunford, A.J. Adeniran, Arch. Biochem. Biophys. 251 (1986) 536.
[40] D. Job, B. Dunford, Eur. J. Biochem. 66 (1976) 607.
[41] J. Kulys, U. Bilitewski, R.D. Schmid, Bioelectrochem. Bioenerg. 16 (1991) 277.
[42] M.H. Smit, A.E.G. Cass, Anal. Chem. 62 (1990) 2429.
[43] J.E. Frew, M.A. Harmer, H.A.O. Hill, S.I. Libor, J. Electroanal. Chem. 201 (1986) 1.
[44] N. Peña, A.J. Reviejo, J.M. Pingarrón, Talanta 55 (2001) 179.
[45] V. Carralero Sanz, M. Luz-mena, A. González-Cortés, P. Yáñez- Seden, J.M. Pingarrón, Anal. Chim. Acta 528 (2005) 1.
[46] H. Anni, T. Yonetani, in: H. Siegel, A. Siegel (Eds.), Marcel Dekker, New York, 1992.
[47] W. Rajesh, K. Takashima, K. Kaneto, React. Funct. Polym. 59 (2004) 163.
[48] Z. Liu, Y. Liu, H. Yang, Y. Yang, G. Shen, R. Yu, Anal. Chim. Acta 533 (2005) 3.
[49] H. Zejli, J.L. Cisnerosc, I. Naranjo-Rodriguezc, B. Liu, K.R. Temsamanib, J.L. Martya, Anal. Chim. Acta 612 (2008) 198.
[50] A.K.M. Kafi, D.Y. Lee, S.H. Park, Y.S. Kwon, Thin Solid Films 516 (2008) 2816.